# Initial tests of new general resistive wall boundary condition

Andrea Montgomery
University of Wisconsin – Madison

with C. C. Hegna, C. R. Sovinec (UW Madison),
S. E. Kruger (Tech-X Corp), and S. A. Sabbagh (Columbia U)

Nimrod Team Meeting – October 27th, 2012 – Providence, RI

# Motivation

- An external wall of finite resistivity plays a major roll in the stability of tokamak devices via a variety of mechanisms:
  - resistive wall mode (RWM): a slow-growing extension of the external kink mode
  - vertical displacement events allowed by resistive wall
  - leaking of external error-fields through the wall, allowing externally driven magnetic islands
  - eddy currents driven in wall which produce a torque on plasma structures, thereby affecting plasma rotation (i.e. through island locking to the wall)
  - resistive wall can be a component of a feedback control scheme
- These mechanisms can be more thoroughly studying by simulating them in an extended MHD code such as NIMROD.

# General resistive wall boundary condition uses numerically determined vacuum field

- Given the location of points on the wall, a Green's function solver (external to NIMROD) determines the vacuum response matrix M, such that for wall locations w:

$$\chi^n(w) = \sum_{w'} M^n(w,w') B^n_{norm}(w')$$

$$\vec{B}^n_{vac} = \nabla \chi^n$$

- This field is then matched across the resistive wall with the perturbed plasma magnetic field calculated by NIMROD to find the n Fourier component of the electric field in the wall.

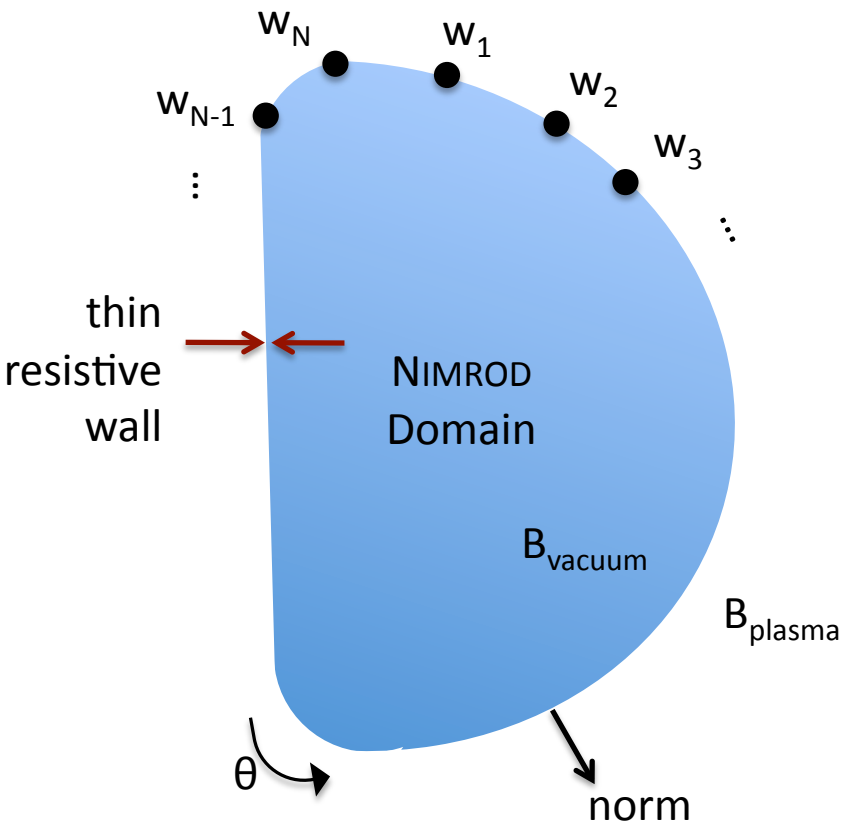


$$\hat{\mathbf{r}} \cdot \left[ \mathbf{B}_{vac} - \mathbf{B}_{plasma} \right] = 0$$

$$\hat{\mathbf{r}} \times \left[ \mathbf{B}_{vac} - \mathbf{B}_{plasma} \right] = \mu_0 \mathbf{K} = \frac{\mu_0 \delta_{wall}}{\eta_{wall}} \mathbf{E}_T$$

# Surface electric field dependent on perturbed plasma fields and χ and its derivatives

- Symmetric toroidal geometry couples poloidal m numbers, but leaves toroidal n numbers decoupled; the general resistive wall boundary condition is consistent with this.

$$\vec{E}^n = v_w \hat{n} \times \left( \nabla \chi^n - \vec{B}^n_{plasma} \right)$$

$$\vec{E}^n = v_w \left[ \left( \frac{-in}{R} \chi + B_{p\phi} \right) \hat{\theta} + \left( \nabla_\theta \chi - B_{p\theta} \right) \hat{\phi} \right]$$

$$v_w \equiv \frac{\eta_{wall}}{\mu_0 \delta_{wall}} \qquad \tau_w \equiv \frac{r_{wall}}{v_{wall}}$$

- Here, θ indicates the direction tangential to the surface in the R-Z plane.
- No-slip velocity boundary conditions are imposed. $\vec{v} = 0$

# A second boundary condition on $B_{norm}$ is required in NIMROD

- An additional boundary condition specifying $B_{norm}$ at the next time step is required because NIMROD uses $\nabla \cdot \vec{B}$ cleaning instead of enforcing $\nabla \cdot \vec{B} = 0$.
- A direct calculation of $\Delta B_{norm}$ from Faraday's law would require second derivatives of χ in the poloidal direction (in the R-Z plane,) which are discontinuous for the numerical expansion used.
- Instead, we use test functions ($\alpha_i$) to create a weak-form surface integral that only requires known derivatives of the test functions.

$$\Delta B_{norm} = -\Delta t \left( \nabla \times \vec{E} \right)_n$$

$$\oint_S \alpha \frac{\Delta B^n_{norm}}{\Delta t} dS = -\oint_S \left[ \nabla \cdot \left( \vec{E}^n \times \alpha \hat{n} \right) + \vec{E}^n \cdot \nabla \times \left( \alpha \hat{n} \right) - \frac{in\alpha}{R} E^n_\theta \right] dS$$

# Boundary condition on $B_{norm}$ uses the weak form of Faraday's law

- The test functions ($\alpha_i$) are the same as the interpolating functions by which each field is represented at nodes within each cell.

$$\oint_S \alpha_i \alpha_j w_j \Delta B^n_{norm,j} dS = \Delta t \oint_S \left[ \alpha_j w_j E^n_{\phi,j} \nabla_\theta \alpha_i + \frac{in}{R} \alpha_i \alpha_j w_j E^n_{\theta,j} \right]$$

- Choosing Gauss-Lobatto-Legendre (GLL) spacing of nodes **and** Lobatto integration for the edge makes the mass matrix on the LHS diagonal, so that the inversion needed to solve for $B_{norm}$ is trivial, and, more importantly, local.
- Gaussian integration works better for regions with steep gradients and changes at cell borders, so the ability to specify different integration schemes for the bulk and the edge has been added.
- As with the second boundary condition for the periodic cylinder, this boundary condition is applied after the matrix solve.

# GLL spacing and Lobatto integration allow for simple mass-matrix inversion

- Positions of interior nodes (with vertices at 0 and 1) are either uniform (default) or Gauss-Lobatto-Legendre (gll, used here)
- Choice of integration scheme (default: Gaussian, here: Lobatto) sets gaussian quadrature points. For Lobatto integration, they are co-located with the gll-spaced nodes and vertices

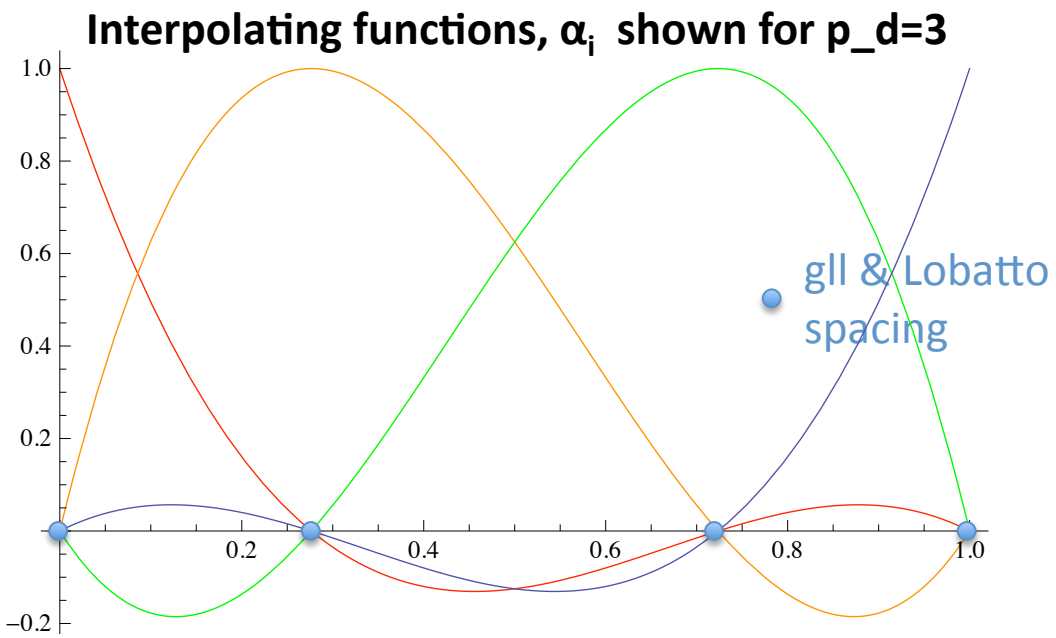


$$\oint_S \alpha_i \alpha_j w_j \Delta B^n_{norm,j} dS = \Delta t \oint_S \left[ \alpha_j w_j E^n_{\phi,j} \nabla_\theta \alpha_i + \frac{in}{R} \alpha_i \alpha_j w_j E^n_{\theta,j} \right]$$

# Original cylindrical boundary conditions and simple equilibrium are used to test new code

- A simple analytic equilibrium modified for use in NIMROD:
  - top-hat current profile modeled as tanh current profile
  - vacuum region between plasma and wall modeled as sparse, resistive region
- Perturb this equilibrium with a $B_r$ eigenfunction proportional to $\cos(2\theta-\phi)$ that has $B_r \neq 0$ at the wall.
- This equilibrium is unstable to a m=2,n=1 RW mode (similar to an external kink.)

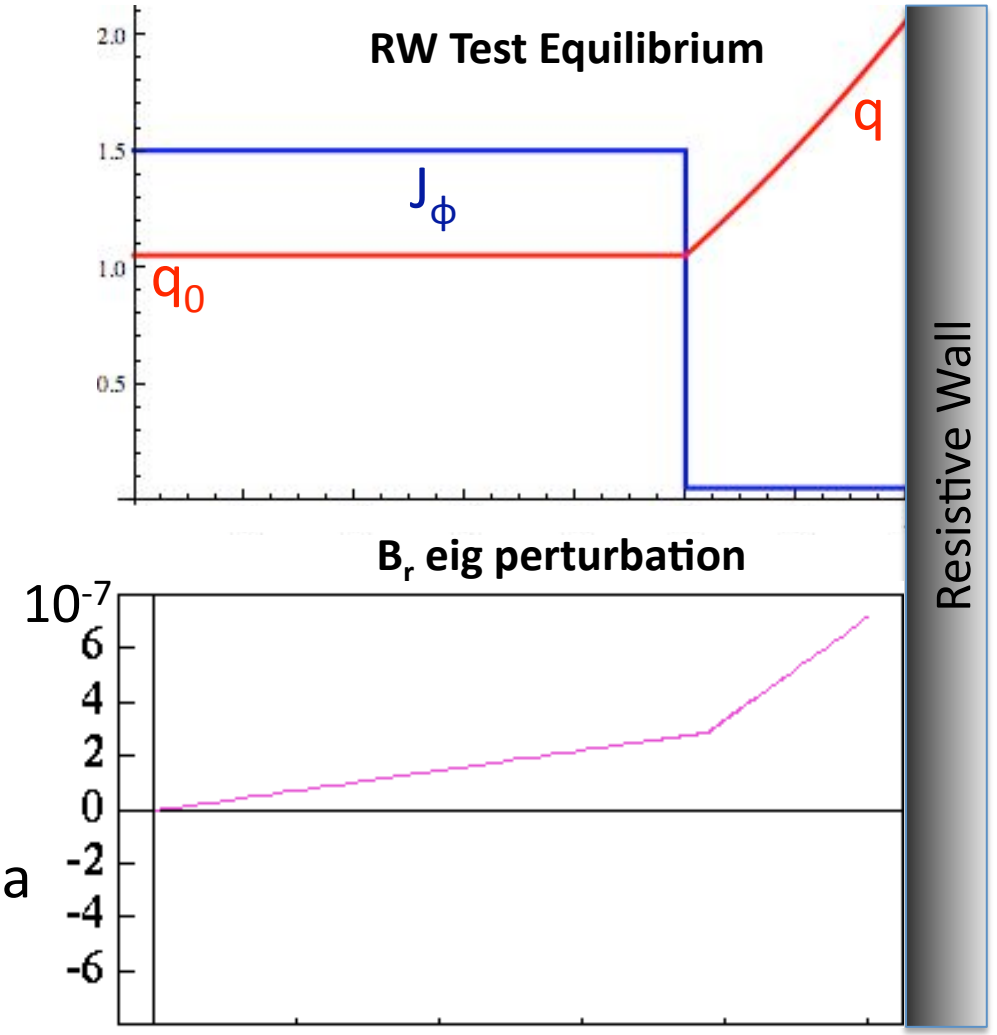

# The vacuum response matrix for a periodic cylinder is used to test new boundary condition

- Using a Green's function method, we can derive the vacuum response matrices for each n in a periodic cylinder:

$$\chi = \left(\overleftrightarrow{I} + \overleftrightarrow{P}\right)^{-1} \overleftrightarrow{Q} B_{norm}$$

$$P_{ij} = 4\pi^2 k r_w \left[2\sum_{m=1}^{\infty} I_m' K_m \cos\left(m\left(\theta_i - \theta_j\right)\right)\right]$$

$$Q_{ij} = 4\pi^2 r_w \left[2\sum_{m=1}^{\infty} I_m K_m \cos\left(m\left(\theta_i - \theta_j\right)\right)\right]$$

- This vacuum response matrix is for n≠0 and m≠0, since we are testing the code for an RWM similar to an external kink.
- Inverse is found using an LU decomposition, and backsubstituting columns of Q to eliminate the need for matrix multiplication.
- These matrices are real, indicating that there is no phase shift between the plasma fields and the vacuum fields.

# Computed growth rate is within 2% of the analytic rate as wall location is varied

$$\%\ \text{error} = 2\frac{\left|\gamma_{analytic} - \gamma_{nimgen}\right|}{\gamma_{analytic} + \gamma_{nimgen}} < 2\%$$

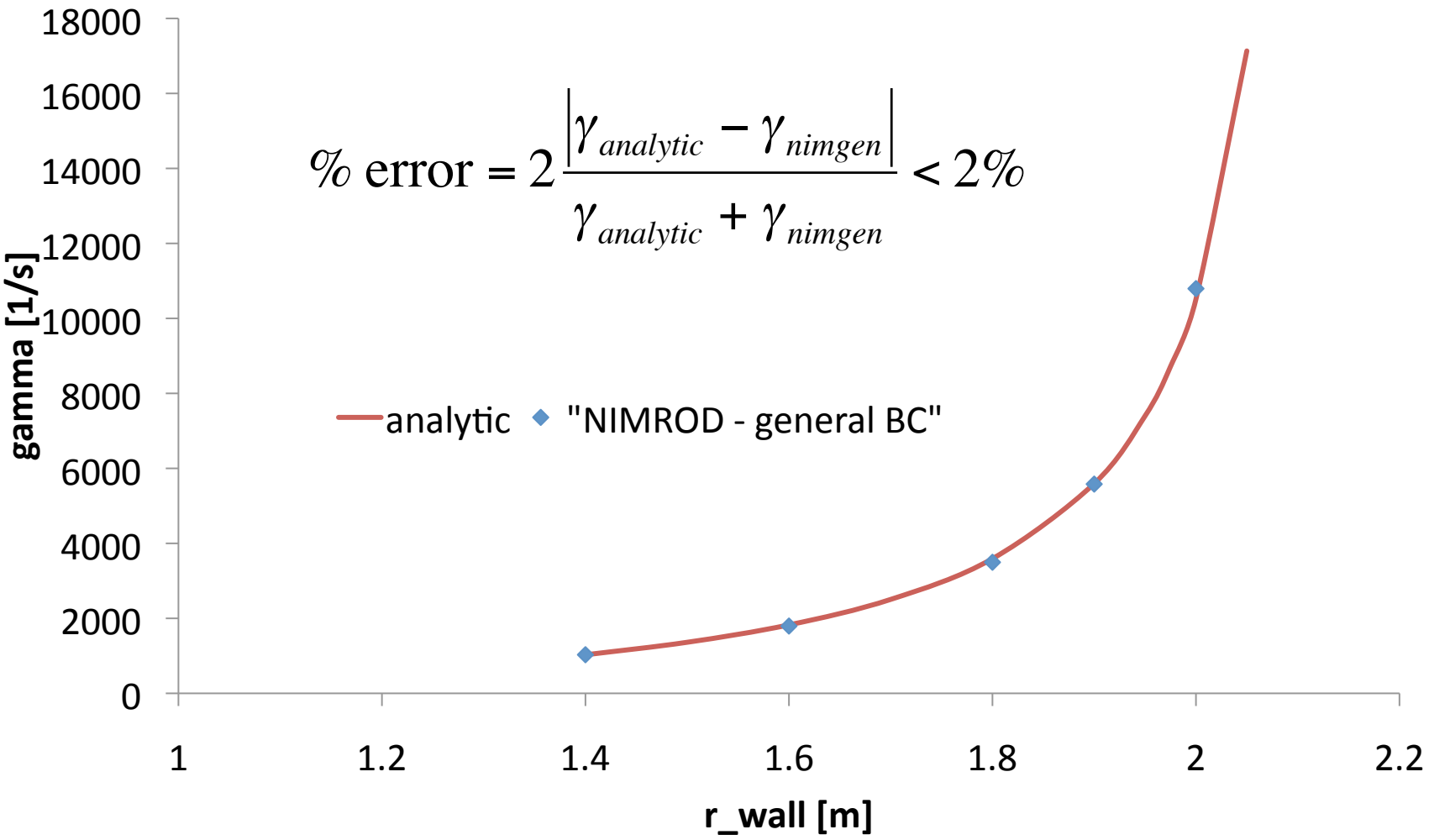

# Magnetic field profiles from new RW boundary condition match original test profiles

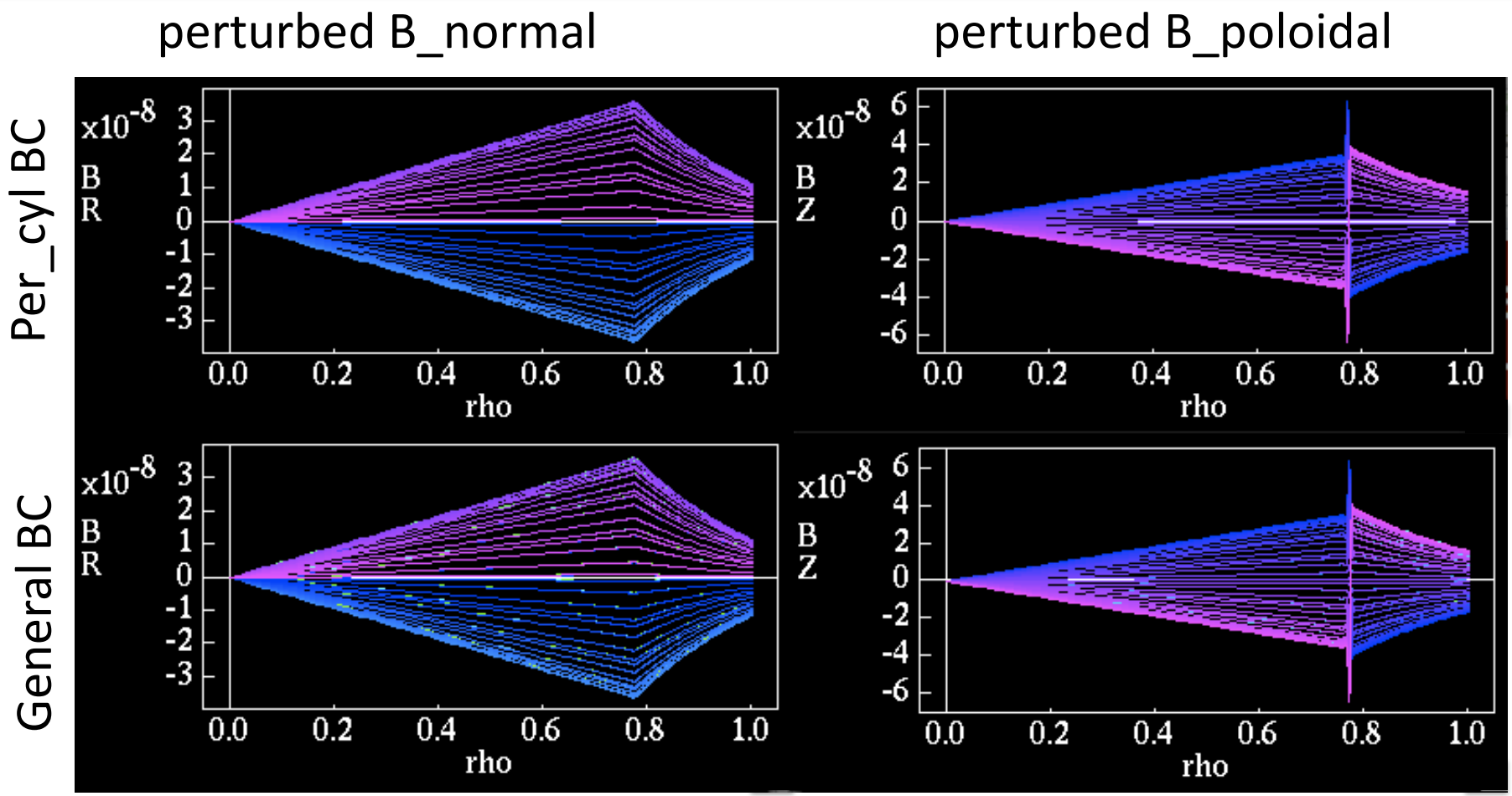


- Magnetic field profiles match analytic predictions for a m=2, n=1 kink-like resistive wall mode, and have $B_r \neq 0$ at the wall.

# Velocity profiles from new RW boundary condition match original test profiles

perturbed V_normal

perturbed V_poloidal

Per_cyl BC

General BC

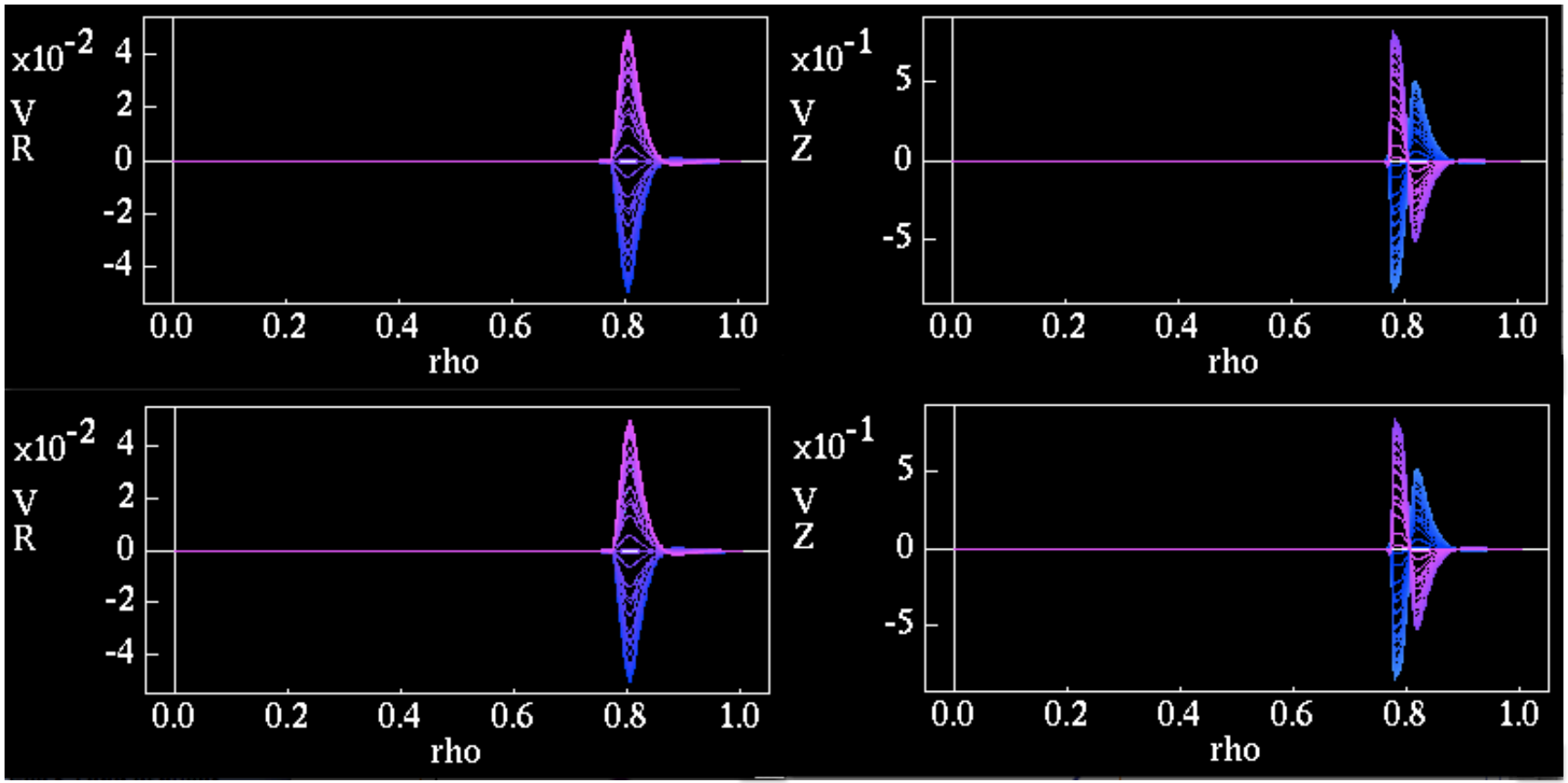


- Spike in velocity profile is due to the plasma column kinking into the vacuum-like region between it and the wall.

# Conclusions

- A full resistive wall boundary condition that can be used for toroidal and cylindrical geometries with coupled m numbers has now been implemented in NIMROD.
- This generalized boundary condition has been tested against theory and previous numerical work for the specific case of a periodic cylinder.
  - Matches analytic growth rates for the RWM to within 2% error.
  - Produces correct eigenfunctions, matching analytic predictions and previous results.

# Future Work

- Test new RW boundary condition running in parallel for periodic cylinder RWM test case
- Examine non-linear evolution of tearing modes with different m numbers as they interact with each other and the wall (for a periodic cylinder).
- Consider how to handle n=0 component of the electric field in the RW for shots with changing plasma current.
- Implement toroidal vacuum response matrix (calculated by GRIN).
- Use smoothed NSTX-like wall with a realistic equilibrium to reproduce vertical displacement events and RWMs.